Journal of Applied Polymer Science

Synergistic effects of crosslinking and chitosan molecular weight on the microstructure, molecular mobility, thermal and sorption properties of porous chitosan/gelatin/hyaluronic acid scaffolds

Cristian A. Acevedo,[1,2] Elizabeth Sánchez,[2] Paulo Díaz-Calderón,[3] Jonny J. Blaker,[4] Javier Enrione,[3] Franck Quero[5]

[1]Departamento de Física, Universidad Técnica Federico Santa María, Avenida España 1680, Valparaíso, Chile
[2]Centro de Biotecnología, Universidad Técnica Federico Santa María, Avenida España 1680, Valparaíso, Chile
[3]Biopolymer Research and Engineering Lab (BiopREL), Universidad de los Andes, Avenida Monseñor Álvaro del Portillo 12.455, Las Condes, Santiago, Chile
[4]Bio-Active Materials Group, School of Materials, The University of Manchester, Manchester, M13 9PL, UK
[5]Departamento de Ciencia de los Materiales, Facultad de Ciencias Físicas y Matemáticas, Universidad de Chile, Beauchef 851, Santiago, Chile
Correspondence to: F. Quero (E-mail: fquero@ing.uchile.cl)

ABSTRACT: In this study, synergistic effects of crosslinking and chitosan molecular weight on the microstructure, molecular mobility, thermal, and sorption properties of porous chitosan/gelatin/hyaluronic acid hybrid foams are reported. Fourier transform infrared spectroscopy has been utilized to confirm the covalent attachment of hyaluronic acid to gelatin and chitosan, and covalent chemical crosslinking between gelatin and chitosan. Detailed image analysis of scanning electron microscopy images of the porous scaffold hydrids reveal that the pore size of the materials formulated using either low- or high-molecular-weight chitosan increases significantly upon crosslinking using ethyl(dimethylaminopropyl) carbodiimide/N-Hydroxysuccinimide. These microstructural changes are even more pronounced for the crosslinked hybrid scaffolds formulated using low-molecular-weight chitosan, highlighting a synergistic effect between crosslinking and the use of low-molecular-weight chitosan. Results obtained using differential scanning calorimetry demonstrate a significant reduction in molecular mobility reduction in molecular mobility for crosslinked scaffolds formed using high-molecular-weight chitosan compared to non-crosslinked hybrids and crosslinked hybrids formulated using low-molecular-weight chitosan. Correspondingly, dynamic vapor sorption evidenced significantly lower water vapor sorption for crosslinked scaffolds formulated using high-molecular-weight chitosan. © 2017 Wiley Periodicals, Inc. J. Appl. Polym. Sci. **2017**, *134*, 44772.

KEYWORDS: biopolymers; chitosan; crosslinking; hybrid; molecular weight; scaffold

Received 21 June 2016; accepted 11 December 2016
DOI: 10.1002/app.44772

INTRODUCTION

Hybrid scaffolds made of gelatin, chitosan, and hyaluronic acid are promising materials to be used for tissue engineering. There is a great interest in developing porous scaffolds with finely controlled microstructures and physical properties suitable for specific tissue engineering applications. There has been significant research effort in bone, skin and cartilage tissue regeneration.[1–3] One tissue engineering strategy consists of seeding cells into porous scaffold materials, which should have specific biological, physical, and chemical properties to stimulate tissue regeneration. A route to tailor materials properties is to combine gelatin, chitosan and hyaluronic acid to form a biopolymer hybrid with unique properties.

Gelatin is a biopolymer with great potential for tissue engineering applications.[4,5] This is because gelatin is directly derived from collagen. The presence of the Arg-Gly-Asp-like amino acid sequence in gelatin has been found to promote cell adhesion and migration.[6] Gelatin, however, is a biomaterial that can provide favorable conditions for bacterial growth. Chitosan has been proven to be biocompatible, biodegradable, nontoxic and to have antibacterial properties.[7–9] As a result, combining gelatin with chitosan allows the creation of a hybrid material with excellent cell adhesion and migration ability as well as antimicrobial activity.[10,11] Furthermore chitosan/gelatin hybrids can form polyelectrolyte complexes, forming an adequate hybrid to culture living cells where they can proliferate and develop cell processes necessary for tissue regeneration.[12] Hyaluronic acid,

naturally present in extracellular matrix (ECM), can be added to chitosan/gelatin hybrids to better mimic ECM. These hybrids have been shown to enhance skin cell growth.[13]

There is still much scope to further tune the physical properties of chitosan-gelatin-hyaluronic hybrid scaffolds to improve the ability of these biomaterials to better regenerate tissues. Some key physical properties of scaffolds that can be fine-tuned include pore morphology,[14–16] molecular mobility,[17] as well as mechanical[16,18] and scaffold/water interaction.[19] Pore morphology is particularly important as it affects cell behavior including proliferation and differentiation. The effect of pore size has been reported to induce cell flattening and to affect the location of cell growth.[14] For example, culture of human trophoblasts in small pore size (~30 μm) 3D nonwoven poly(ethylene terephthalate) (PET) fibrous matrix was found to limit the formation of large cell aggregates and reduce cell differentiation compared to PET fibrous matrix having larger pore size (~39 μm).[20] Consequently, the design of porous scaffolds having bigger pore size diameter could provide better cell aggregation and differentiation. As for the molecular mobility, it also plays a key role in cell growth. It has been reported in gelatin-containing scaffolds that when they contain polymers with high mobility, their ability to stimulate cell growth is five times less efficient compared to scaffolds where the polymer mobility is more restricted.[17] Tuning the mechanical properties of scaffolds has also been found to be relevant for successful tissue regeneration.[18] The effect of stiffness on the cell number and differentiation in collagen-glycoaminoglycan scaffolds was investigated. It was found that scaffold stiffness has different effects on differentiation and proliferation.[18] Scaffolds of lower stiffness were found to promote cell mediated contraction, which had a positive effect on the modulation of osteoblasts differentiation and reduced cell numbers.[18] The water uptake of chitosan/nanohydroxyapatite scaffolds formulated using high molecular weight (MW) and medium MW chitosan was found to be relevant to provide dimensional stability to the scaffolds during cell culture. It was found that a scaffold formulation containing high MW chitosan as well as 1% nanohydroxyapatite significantly reduced water uptake and therefore provided better dimensional stability compared to other scaffold formulation including when using medium MW chitosan.[19] This highlights the importance of selecting chitosan with the relevant MW but also that controlling scaffold water interaction in scaffolds for optimized tissue regeneration. Consequently by controlling pore size, molecular mobility, mechanical and scaffold/water interaction, one may fine-tune the structure and so optimize the regenerative ability of porous scaffolds to be used for tissue engineering applications.

MW is a very important characteristic of polymers and it needs to be controlled to optimize their physical properties including molecular mobility, thermal and sorption properties. It has been reported that the physical properties of chitosan scaffolds exposed to microwave irradiation are dependent on MW.[21] Microwave irradiation was found to significantly reduce chitosan molecular weight, which induced a significant decrease in crystallinity, exothermic peak temperature and swelling ratio. Moreover, the effect of chitosan MW on the physical properties of nanocellulose-containing composites has been previously studied.[22] This effect was found to show remarkable potential for formulating blends and composites.[22] The effect of using chitosan with different MW on the physicochemical properties of fish gelatin-based films has been previously reported.[23] Fish gelatin showed stronger interaction with high MW chitosan compared to low MW chitosan, promoting improved mechanical properties including higher tensile strength and elongation at break.[23] Other physical properties including gel strength and glass transition temperature were significantly increased upon the use of high MW chitosan. Water vapor permeability was, however, significantly reduced. As a result, chitosan MW could potentially affect the physical properties of chitosan/gelatin hybrid porous scaffolds.

This study aims to understand the combined effects of crosslinking and chitosan MW on the microstructure, molecular mobility, thermal and sorption properties of chitosan/gelatin/hyaluronic acid scaffolds. This may be a route to further optimize and fine-tune their structure and properties for specific tissue engineering applications. Upon crosslinking, these scaffolds were previously found to be water–insoluble and despite the fact they were crosslinked, the scaffold materials were found to be biodegradable *in-vivo* when applied for wound healing application.[2]

EXPERIMENTAL

Materials and Chemicals

Bovine gelatin (bloom 200, pharmaceutical grade) was purchased from Merck (Germany). Chitosan (pharmaceutical grade) with molecular weights of 120 and 300 kDa (derived from crab shells, 85% deacetylated), were purchased from Quitoquimica (Chile). Hyaluronic acid (medical grade, 980 kDa) was purchased from Lifecore Biomedical LLC (USA). EDC (1-ethyl-(3,3-dimethylaminopropyl)-carbodiimide), NHS (N-hydroxysuccinimide) and MES (2-morpholine-ethane sulfonic acid) were purchased from Sigma-Aldrich (USA).

Fabrication and Crosslinking of Porous Scaffolds

Chitosan/gelatin/hyaluronic acid scaffolds were prepared using a freeze-drying method previously described in the literature.[13] After freeze-drying, the hybrids were subsequently crosslinked using the often used EDC/NHS crosslinking system.[24] Chitosan/gelatin/hyaluronic acid scaffolds have been previously tested *in-vitro* and *in-vivo*.[2,13] They also have been reported to be suitable after radiation sterilization for tissue engineering purposes.[24]

Chitosan/gelatin/hyaluronic acid formulations were produced by mixing chitosan (2 w/v % in 1 w/v % acetic acid), gelatin (1 w/v % in water) and hyaluronic acid (0.01 w/v % in water) at 50 °C corresponding to a rationale formulation of chitosan/gelatin/HA of 2:7:1. The solution was then poured into a Petri dish adjusting its volume to obtain a height of ~3 mm. The poured mixtures were subsequently cooled down to 4 °C for 12 h to obtain a hydrogel and subsequently frozen at −80 °C for 24 h. The materials were then immersed in liquid nitrogen and lyophilized for 48 h using a freeze dryer (Labconco, USA). Half of the freeze-dried chitosan/gelatin/hyaluronic acid hybrids were then crosslinked at room temperature by immersion for 2 h into a solution

comprising 30 mM EDC and 8 mM NHS, using ethanol 90 v/v % as solvent and MES (50 mM) as buffer. The resultant crosslinked matrix was then washed three times with ethanol to remove unreacted EDC, NHS and MES. Crosslinked scaffolds were then refrozen and freeze-dried (as previously described). The final composition of the freeze-dried hybrid scaffold materials was 36.3 w/w % of chitosan, 63.6 w/w % of gelatin and 0.1 w/w % of hyaluronic acid (based on dried weight).

Characterization of Chitosan/Gelatin/Hyaluronic Acid Hybrid Scaffolds

FTIR Assessment of Molecular Structure and Crosslinking. A Fourier transform infrared (FTIR) spectrometer (Nicolet 5700, Thermo Electron Co-operation, USA) was used to collect the spectra of all hybrid scaffold material compositions. Spectra were recorded in the wavenumber range of 900 to 1800 cm^{-1} with a resolution of 4 cm^{-1} and 32 scans. Measurements were performed in triplicate on different areas of the sample and the most representative result is presented. All the spectra were baseline corrected and normalized with respect to the Amide I band as previously reported before for gelatin and gold gelatin nanocomposites.[25,26] This band was the highest intensity band over the considered wavenumber range. Consequently the intensity of the Amide I band was not considered for spectra interpretation.

Pore Morphology by SEM. The microstructure of the chitosan/gelatin/hyaluronic acid hybrid scaffolds was observed using a Carl Zeiss SEM (EVO *MA* 10, Germany), at an acceleration voltage of 25 kV. Samples were previously gold-coated (10–20 nm) using a diode magnetron sputter coater (SPI Sputter Coater model 12161, USA).

The pore size (equivalent circle diameter) of chitosan/gelatin/hyaluronic acid scaffolds was estimated from SEM image analysis by using the ImageJ software (NIH, USA) from at least 100 pores per scaffold. Averages and their associated standard errors are reported. Significance of the results was evaluated using Student's *t*-test.

Molecular Mobility and Thermal Properties by DSC. Prior to the analysis, all samples were equilibrated (up to reaching constant weight) in a chamber at 75% relative humidity (using a NaCl saturated solution). Then, each sample of ~15 mg was hermetically sealed in an aluminum pan.

The thermal properties of all hybrid scaffold material compositions were determined by DSC (Mettler Toledo DSC 1 STARe System, Switzerland) using a heat-cool regime starting from −20 °C to 130 °C, holding at 130 °C for 1 min, cooling to −20 °C, all at 10 °C min^{-1}. The device was previously calibrated using indium as a standard ($T_{m\ onset}$ = 156.6 °C; ΔH_m = 28.5 J g^{-1}), and empty pan was used as reference.

The melting temperatures (T_m) of non-crosslinked and crosslinked hybrids, equilibrated at 75% relative humidity, were determined as the onset of the endothermic peak observed on the first heating scan. The enthalpy of melting (ΔH_m) was calculated as the area under the melting peak. The glass transition temperature (T_g) was determined as the mid-point of the inflection point of the change in heat capacity. The T_g was used as an indicator for molecular mobility. Experiments were performed in triplicate and averages and standard deviations are reported.

Scaffold/Water Interaction by DVS. Moisture sorption isotherms of the hybrid scaffold materials were determined by dynamic vapor sorption (DVS Intrinsic, Surface Micro Systems, USA). The sorption was recorded by measuring sample mass as a function of time. The sample was typically equilibrated at a constant temperature at various relative humidities, which are stated by changing the gas humidity (a mixture of dry and moisture-saturated nitrogen), flowing over the sample at 200 cm^3 min^{-1}. Specifically the programmed equilibrating relative humidity used was from ~0 to 90% with 10 increments (10 points) at 20 °C. ~10 mg of hybrid scaffold was used for each experiment, and equilibrium considered to be reached when *dm/dt* (change in mass over time) was < 0.002%/min.[27] If the sorption equilibrium was not reached within the experiment time-scale (8 h), an exponential function was used to extrapolate the moisture content at time equal to infinity following the methodology described previously in the literature.[28]

The moisture sorption isotherms were fitted by the Guggenheim, Anderson and de Boer (GAB) equation[29–31]:

$$M = \frac{m_0\ CKa_w}{(1-a_w)(1-Ka_w+CKa_w)} \quad (1)$$

where M is the moisture content of the hybrid materials (%, dry basis) and m_0 is the monolayer value (%, dry basis). C is related to the energy associated with the interaction between water molecules and the matrix primary interaction sites or monolayer. K is also a temperature-dependent parameter related to the heat of sorption at the multilayer, and a_w represents the water activity (RH/100). Fitting was performed by minimization of the quadratic difference between the experimental and predicted values using the Solver package in Excel (Office 2007, Microsoft Corp.). The fitting error was evaluated using the equation of Mean Relative Error (MRE):

$$\mathrm{MRE} = \frac{100}{n}\sum_{i=1}^{n}\frac{|X_{ei}+X_{pi}|}{X_{ei}} \quad (2)$$

where X_{ei} is the experimental value, X_{pi} is the predicted value and n is the number of experimental data. MRE values ≤ 10% were considered as a good fit to the experimental data.[32] The MRE values corresponding to the various scaffold formulation were 0.90, 1.81, 1.25 and 2.29 for the scaffolds formulated with respectively non-crosslinked high MW chitosan, crosslinked high MW chitosan, non-crosslinked low MW chitosan y crosslinked low MW chitosan.

RESULTS AND DISCUSSION

Molecular Composition and Crosslinking

FTIR was used to identify the molecular composition and demonstrate the crosslinking of chitosan/gelatin/hyaluronic acid hybrids using EDC/NHS crosslinking agent. Also, FTIR was utilized to observe possible difference in the spectra obtained from the materials formulated using low- and high-MW chitosan. The crosslinking reaction between chitosan and gelatin has been described and reported before in the presence of EDC, NHS and hyaluronic acid.[33,34] This reaction induces the formation of C—O bonds as well as the formation of aliphatic C—N bonds,

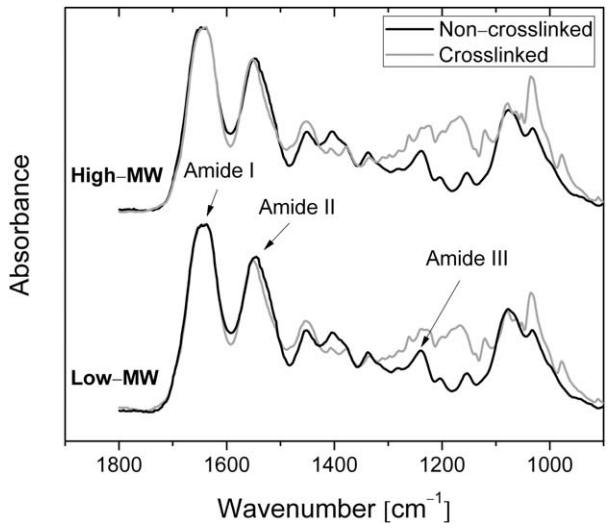

Figure 1. Typical normalized ATR FTIR spectra obtained for non-crosslinked and crosslinked chitosan/gelatin/hyaluronic acid scaffolds prepared with low- and high-molecular-weight (MW) chitosan in the wavenumber range of 1800 to 900 cm^{-1}.

leading to covalent crosslinking of gelatin and chitosan as well as covalent bonding of hyaluronic acid to gelatin and chitosan.

Figure 1 reports typical FTIR spectra obtained in the wavenumber range of 1800 to 900 cm^{-1} for non-crosslinked and crosslinked chitosan/gelatin/hyaluronic acid scaffolds prepared using low- and high-MW chitosan. From these spectra, as expected, the gelatin contribution dominates the overall signal due to the higher concentration of gelatin (~63.6 wt/wt %) present in the chitosan/gelatin/hyaluronic acid hybrids compared to the concentration of chitosan (~36.3 wt/wt %) and hyaluronic acid (~0.1 wt/wt %). As reported in Table I, all hybrid materials display the typical Amide I, II and III bands, which are characteristic of gelatin and chitosan.[34] Comparing spectra obtained from non-crosslinked and crosslinked chitosan/gelatin/hyaluronic acid scaffolds the intensity of the Amide II band did not significantly change. With respect to the amide III band for the crosslinked scaffolds, one can observe the overlapping of two peaks, with one being the contribution of the amide III band. The contribution to the intensity of the Amide III band in the crosslinked scaffolds, however, significantly decreases upon crosslinking despite a change of baseline. This change of peak intensity is likely to arise from the reaction of free NH_2 moieties belonging to gelatin and chitosan, possibly due to the formation of aliphatic C—N bonds. This observation suggests the formation of covalent bonding between gelatin and chitosan but also between hyaluronic acid and gelatin as well as chitosan.[33] This decrease in intensity of the Amide III band has never been reported in previous works focusing on the crosslinking of chitosan/gelatin/hyaluronic acid hybrids crosslinked with EDC/NHS[33] and EDC.[34] In these two works, the intensity of the Amide I bands was found to subtly increase upon crosslinking, which was attributed to an increase in the number of N—H bonds. In another work, a decrease in intensity of the amide II band was reported and attributed to the conversion of —NH_2 moeities in N—H bonds.[39] With respect to comparing FTIR spectra from non-crosslinked and crosslinked hybrids formulated either using low- and high-MW chitosan, no difference is noted, which could originate from the lower weight fraction of chitosan (~36.3 wt/wt %) introduced in the hybrid materials compared to gelatin (~63.6 wt/wt %).

Figure 2 reports typical FTIR spectra obtained for non-crosslinked and crosslinked chitosan/gelatin/hyaluronic acid scaffolds prepared using low- and high-MW chitosan in the wavenumber range of 1300 to 1000 cm^{-1}. As previously mentioned, during the chemical reaction between the carboxylic groups of hyaluronic acid and gelatin with EDC, C—O bonds are formed and are related to the presence of an FTIR band located at 1078 cm^{-1}.[33] In the present study, two bands, observed for the crosslinked hyaluronic acid scaffolds, located at 1078 and 1120 cm^{-1} suggest the formation of C—O bonds between hyaluronic acid and gelatin, which is related to the formation of ester C—O linkages.[33,36,40] The interpretation for the presence of a sharp peak located at 1078 cm^{-1} needs, however, a more precise interpretation. For the uncrosslinked scaffolds, one can observe the presence of a broad FTIR band located close to the wavenumber position of 1078 cm^{-1}. The presence of a sharp FTIR band located at 1078 cm^{-1} for the crosslinked scaffolds is attributed to formation of C—O linkages. This sharp FTIR band located at 1078 cm^{-1} actually overlaps with the broad FTIR band that had a higher intensity for the non-crosslinked scaffolds compared to the crosslinked scaffolds.

Figure 2 and Table I report the presence and position of additional FTIR bands for crosslinked chitosan/gelatin/hyaluronic acid scaffolds in the wavenumber range of 1300 to 1000 cm^{-1}. FTIR bands corresponding to the stretching vibration of aliphatic C—N bonds, in polymers, have been reported to occur in the wavenumber range of 1020 to 1250 cm^{-1} [41] and 1000 to 1400 cm^{-1}.[42] These bands have been reported to have medium to low weak intensity.[41] The presence of those bands for the hybrid materials, reported in the present study, may be a further indication of covalent reaction of hyaluronic acid with gelatin and chitosan as well as crosslinking between gelatin and chitosan. The presence of these FTIR bands has never been reported before and provides new insights in the molecular structure of crosslinked chitosan/gelatin/hyaluronic acid scaffolds compared to what has been previously published for hybrid scaffolds crosslinked with EDC and EDC/NHS.[33,34] FTIR bands, located in the wavenumber range of 1000 to 1300 cm^{-1} demonstrate the possible formation of C—O and aliphatic C—N bonds expected during the crosslinking reaction between chitosan, gelatin and hyaluronic acid in the presence of EDC.[33] Again, in that wavenumber range, no difference is noted when comparing FTIR spectra from non-crosslinked and crosslinked hybrids formulated using either low- or high-MW chitosan. Figure 3 summarizes the crosslinking mechanism of chitosan/gelatin/hyaluronic acid scaffolds using the EDC/NHS crosslinking system.

Porous Morphology of Scaffolds

Figure 4 reports typical SEM images obtained for noncrosslinked and crosslinked chitosan/gelatin/hyaluronic acid hybrid scaffolds prepared using low- and high-MW chitosan. From these images, no significant difference is observed between the

Table I. Band assignments from ATR-FTIR spectrum from non-crosslinked and crosslinked chitosan/gelatin/hyaluronic acid scaffolds prepared using low- and high-molecular-weight chitosan. Sym, asym, ν, δ refer to symmetric, asymmetric, stretching and bending respectively

Non-crosslinked chitosan/ gelatin/hyaluronic acid	Region	Position [cm^{-1}]	Assignment	Reference
	Amide I	1633	νC=O, νNH	34
	Amide II	1540	δNH, νC—N, νC—C	34
		1400	sym νCOO—	34
	Amide III	1234	νC—N, δNH	34
	Saccharide	1149	asym νC—O—C	34
	Saccharide	1068	Skeletal νC—O	34
	Saccharide	1029	Skeletal νC—O	34
	Saccharide	906	δCH β-glycosidic bond	34
Crosslinked chitosan/gelatin/ hyaluronic acid				
	Amide I	1635	νC=O, νNH	34
	Amide II	1546	δNH, νC—N, νC—C	34
		1403	sym νCOO—	34
		1261	asym νC—N	35
	Amide III	1245	νC—N, δNH	34
		1218	asym νC—N	35
		1198	sym νC—N	35
		1120	νC—O	36
		1078	νC—O	33
	Saccharide	1066	Skeletal νC—O	34
		1051	νC—N	37
		1034	νC—N	38
	Saccharide	906	δCH β-glycosidic bond	34

porous structures of the non-crosslinked and crosslinked scaffolds formulated using high or low MW chitosan. A finer image analysis on the pore size of the scaffolds was, however, carried out. Detailed information on the pore sizes are given in Table II. From this analysis, it is evident that the pore size of crosslinked chitosan/gelatin/hyaluronic acid scaffolds is larger than their counterparts, particularly when crosslinked hybrids were formulated using low-MW chitosan. Scaffolds with significantly bigger pore sizes can be consequently obtained owing to a synergistic effect between crosslinking and with the use of low-MW chitosan.

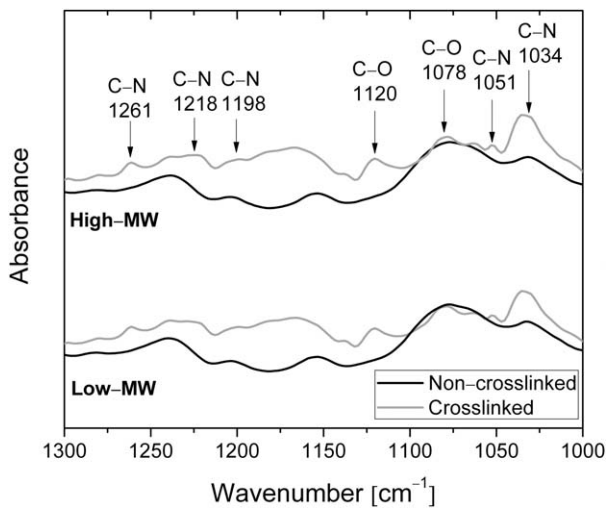

Figure 2. Typical normalized ATR FTIR spectra obtained for non-crosslinked and crosslinked chitosan/gelatin/hyaluronic acid scaffolds prepared with low- and high-molecular-weight (MW) chitosan in the wavenumber range of 1300 to 1000 cm^{-1}.

The EDC/NHS crosslinking agent significantly increases ($p < 0.01$, *t*-test) the pore size of the scaffold and the difference is even more pronounced when the scaffolds are formulated using low-MW chitosan. Obtaining porous scaffolds with bigger pore size diameter could be particularly interesting to promote larger cell aggregates as well as improved cell differentiation.[20] It is likely that the growth of ice crystals during freezing of hybrid scaffolds containing high-MW chitosan is slower than when formulated using low-MW chitosan, which on freeze-drying form larger pores in the low-MW chitosan hybrid scaffolds as reported in Table II. The ice crystal formation may be slowed down due to the possible higher viscosity of high-MW chitosan compared to low-MW chitosan. There is, however, no direct evidence of this in the present study. It is important to highlight that the morphology of the chitosan/gelatin/hyaluronic acid scaffold changes upon chemical reaction using EDC/NHS, affecting not only the molecular structure (producing covalent

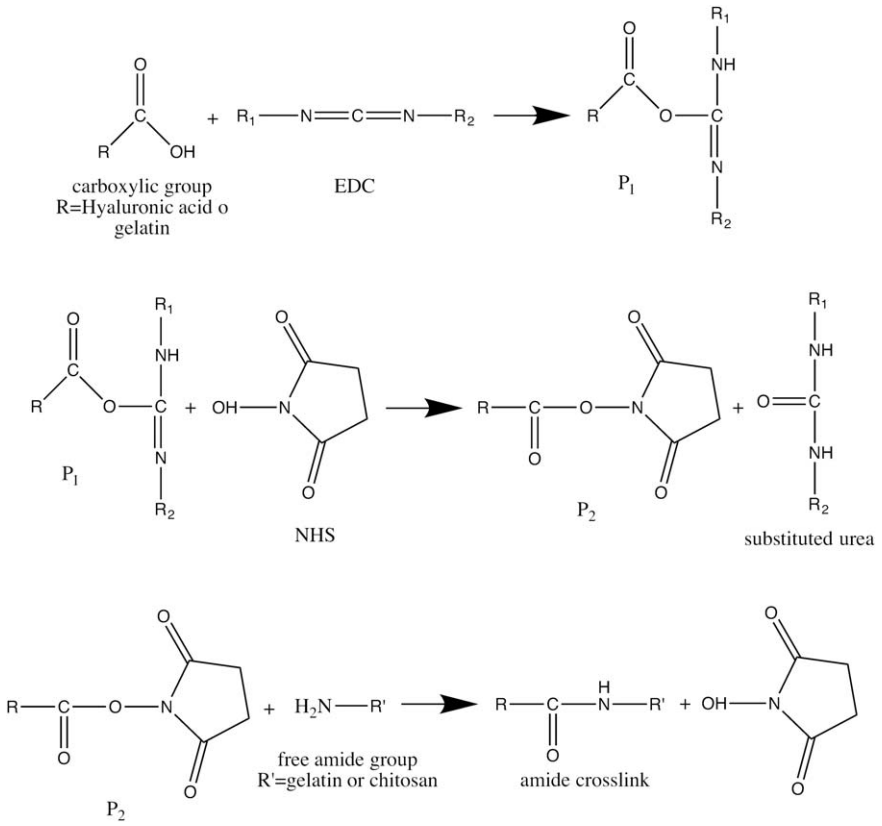

Figure 3. Schematic representation of the formation of covalent bonds between gelatin, chitosan and hyaluronic acid in the presence of EDC and NHS. Reproduced with modification from.[33]

bonding), but also creating a new microstructure with larger pore sizes. The latter is interesting in the application of these materials for tissue engineering application. The interaction between the cells and the scaffold depends on the pore size and how it changes after the preparation.[43]

Molecular Mobility and Thermal properties

Figure 5 reports typical DSC traces for non-crosslinked and crosslinked chitosan/gelatin/hyaluronic acid scaffolds prepared with low- and high-MW chitosan. For non-crosslinked materials, the glass transition temperature (T_g) is observed at ~42 °C and the endothermic peak at ~80 °C. A single T_g can be observed in all scaffolds, suggesting relatively good miscibility between the gelatin and chitosan during their preparation and processing. Thermal properties obtained from DSC measurement are summarized in Table II. Comparing the T_g values for non-crosslinked and crosslinked chitosan/gelatin/hyaluronic acid scaffolds, a small but significant shift ($p < 0.05$) to a higher temperature is only observed for the crosslinked formulation containing high-MW chitosan, likely due to reduced mobility within the scaffold materials owing to chemical crosslinking. This means that the crosslinked scaffolds formulated using high-MW chitosan have a reduced mobility compared to crosslinked scaffolds formulated using low-MW chitosan. This is supported by DSC data where a small but significant increase of T_g ($p < 0.05$) was measured for crosslinked scaffold materials formulated with high-MW chitosan. Another contribution to this may arise from possible higher level of hydrogen bonding interactions between gelatin and high-MW chitosan compared to with low-MW chitosan. This highlights a synergistic effect on the scaffold molecular mobility when it is both crosslinked and formulated using high-MW chitosan. This synergistic effect may originate from enhanced level of hydrogen bonding interaction between gelatin and high-MW chitosan.[23]

Small but significant changes in T_m ($p < 0.05$), probably mostly originating from the gelatin fraction, were also observed between non-crosslinked and crosslinked scaffold materials. The presence of an enthalpy of melting is indicative of the presence of crystalline fractions in the hybrid scaffold materials. Even in the presence of crosslinks, an enthalpy of melting could still be observed although its value was significantly lower than for the non-crosslinked scaffolds. Due to crosslinking, the T_m and enthalpy of melting of crosslinked hybrid scaffold materials were significantly lower than for the non-crosslinked materials. This may be directly related to the presence of crosslinks that possibly restricts both the formation of the triple-helix configuration in the gelatin fraction on cooling and possibly of the crystalline fraction of chitosan. This is because the presence of both crystalline fractions is proportional to the enthalpy of melting. This observation has never been reported before for chitosan/gelatin/hyaluronic acid scaffolds and provides new insights in the amorphous/crystalline structure of these scaffold materials.

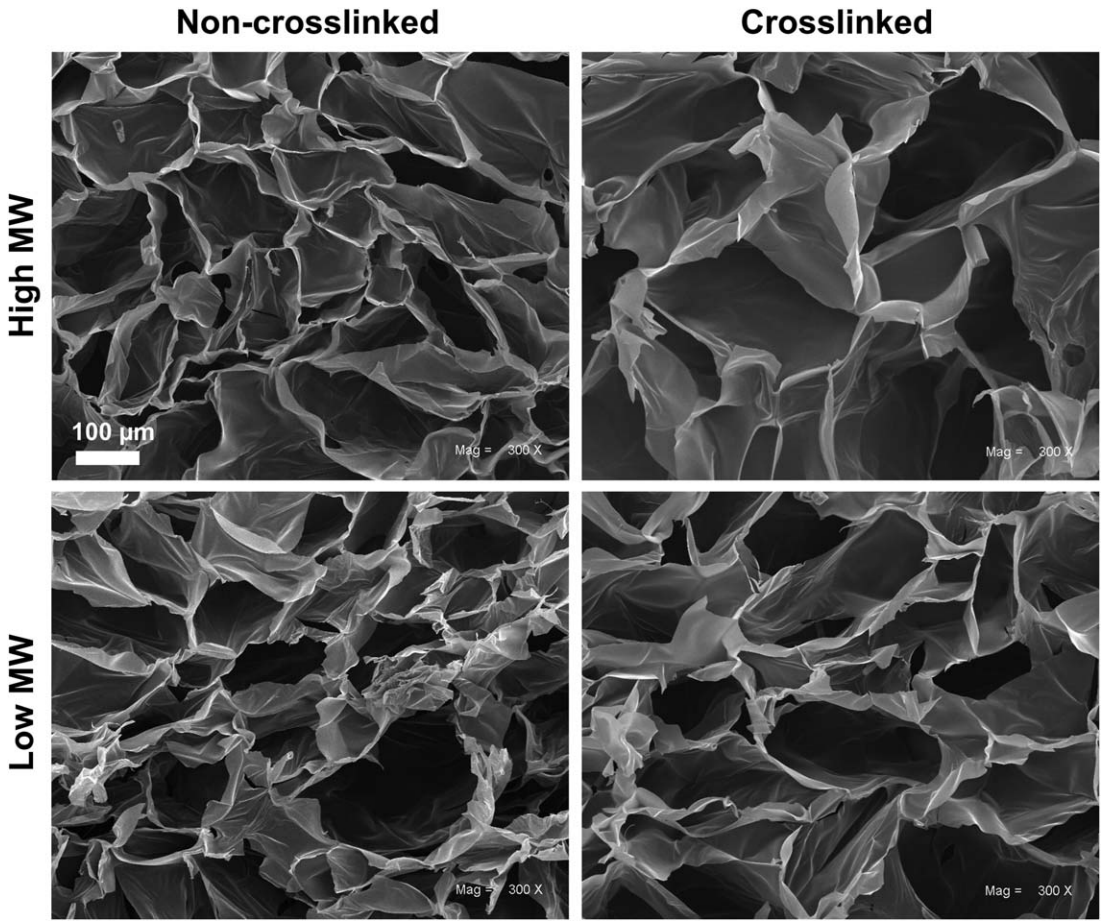

Figure 4. Typical scanning electron micrographs obtained for non-crosslinked and crosslinked chitosan/gelatin/hyaluronic acid scaffolds prepared with low- and high-molecular-weight (MW) chitosan. The bar size is the same for all images.

Scaffold/Water Interaction

Figures 6(a,b) report typical water sorption curves obtained for non-crosslinked and crosslinked chitosan/gelatin/hyaluronic acid scaffolds prepared with low- and high-MW chitosan respectively. All sorption curves show typical sigmoidal shape (isotherm type II) belonging to multilayer molecular adsorption phenomenon in porous surfaces, with a characteristic pattern for polymer-based matrices holding small amount of water at low relative humidity and large amounts at high relative humidity levels.[44] Conversely, both plots show a decrease in moisture content when the scaffold sample is crosslinked. This suggests that linkages between the polymer chains result in less available polar sites for bonding water. Significant decrease in moisture was observed in a relative humidity range of 30–90% in

Table II. Scaffold physical and thermal properties: Pore size, glass transition temperature (T_g), melting temperature (T_m), enthalpy of melting (ΔH_m), monolayer value (m_0), energy associated with the interaction between water molecules and the matrix primary interaction sites or monolayer (C) and temperature-dependent parameter related to the heat of sorption at the multilayer (K) of non-crosslinked and crosslinked chitosan/gelatin/hyaluronic acid scaffolds prepared with low- and high-molecular-weight chitosan

	High-MW		Low-MW	
	Non-crosslinked	Crosslinked	Non-crosslinked	Crosslinked
Pore size [µm]	94.8 ± 1.7	107.7 ± 2.6	99.3 ± 1.7	123.4 ± 2.7
T_g (°C)	41.6 ± 0.3	46.0 ± 1.7	41.6 ± 0.01	42.1 ± 1.4
T_m (°C)	78.7 ± 2.5	61.7 ± 0.6	79.4 ± 1.9	63.9 ± 0.5
ΔH_m [J/g]	16.6 ± 0.3	7.3 ± 0.9	17.2 ± 0.5	8.8 ± 0.3
m_0 [%]	9.7 ± 0.9	6.9 ± 1.8	9.5 ± 1.3	7.9 ± 2.3
C	4.0	5.2	6.1	4.2
K	0.8	0.9	0.8	0.9

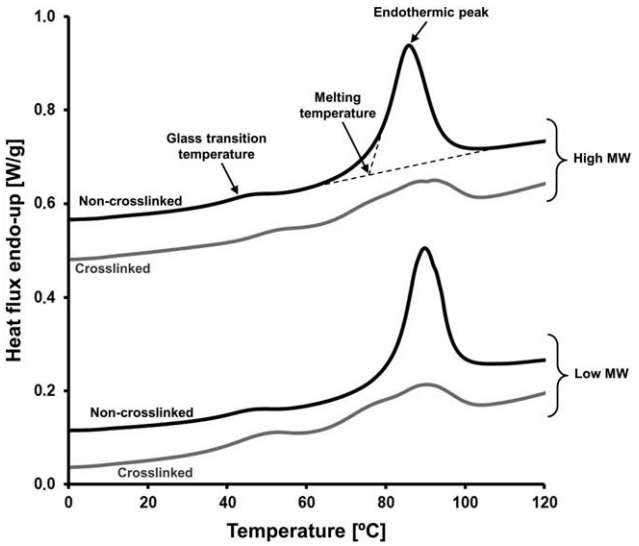

Figure 5. Typical first heating curves obtained by differential scanning calorimetry for non-crosslinked and crosslinked chitosan/gelatin/hyaluronic acid scaffolds prepared with low- and high-molecular-weight (MW) chitosan.

scaffolds prepared with high-MW chitosan, and in a relative humidity range of 10–60% in scaffolds with low-MW chitosan. Small but significant differences between non-crosslinked chitosan/gelatin/hyaluronic acid scaffolds and crosslinked chitosan/gelatin/hyaluronic acid scaffolds prepared using low-MW chitosan are, however, observed. The use of low or high-MW chitosan when formulating non-crosslinked hybrid scaffold materials was not sufficient to induce significant reduction in moisture content. A similar conclusion can be drawn for the crosslinked scaffold materials, formulated using low-MW chitosan. The combination of crosslinking and the use of high-MW chitosan, however, resulted in significant reduction in moisture content of the scaffolds materials, over the whole equilibrated relative humidity range of 0–90%. This synergistic effect on the moisture content was found to be even stronger in the relative humidity range of 70 to 90%. This result is relevant to limit the plasticizing effect of water which can affect the mechanical properties of the scaffolds and so the proliferation and differentiation of cells.[18] This reduced sorption capacity is also relevant to provide improved dimensional stability to the scaffolds when exposed to body fluids.

The fact that non-crosslinked scaffolds showed higher moisture sorption is well supported by GAB parameters as reported in Table II. The monolayer moisture content (m_0, %) of non-crosslinked scaffolds is higher than crosslinked scaffold (9.5% and 9.7% for low- and high-MW chitosan, respectively) supporting the idea of reduced polar site availability for association with water in the crosslinked scaffolds. With respect to the K value (a temperature-dependent parameter related to the heat of sorption at the multilayer), and increase in the GAB constant tending to 1 (0.9 in both crosslinked scaffolds), suggests a smaller difference between the energy associated with the heat of sorption of the multilayer and the heat of condensation of pure water. The increase in this value indicates a reduction in sorption energy of the multilayer as demonstrated before for mixtures of starch and glycerol.[27] In the present study, this is probably mostly due to the crosslinking process and possibly due to an increased level of hydrogen bonding formation between gelatin and high-MW chitosan. This is in agreement with lower m_0 value obtained from those samples. The C value (constant related to the energy associated with the interaction between water molecules and the matrix primary interaction sites or monolayer), however, does not follow a clear trend.

The lower moisture contents of crosslinked scaffolds as shown by sorption curves and GAB parameters are in agreement with the presence of bands of FTIR spectra indicating covalent reaction of hyaluronic acid with gelatin and chitosan as well as crosslinking between gelatin and chitosan, as previously discussed. Similar conclusion can be drawn with respect to thermal properties, where lower values of melting enthalpy could be reflecting less ability of gelatin chains to fold and recover their triple-helix configuration due to crosslinking, promoting reduced interaction with water and hence lower moisture content. Interestingly, these results suggest that water-scaffold

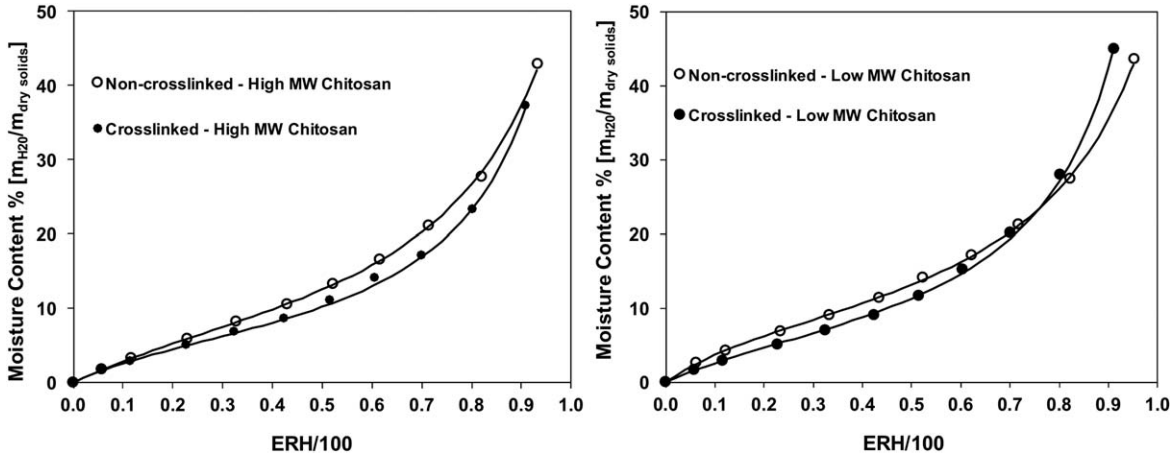

Figure 6. Typical sorption curves obtained by dynamic vapor sorption for non-crosslinked and crosslinked chitosan/gelatin/hyaluronic acid scaffolds prepared with high- (a) and low- (b) molecular-weight (MW) chitosan. ERH stands for equilibrium relative humidity. Solid lines correspond to GAB fitting at 20 °C.

interaction is not driven by the microstructure morphology. This is because in both crosslinked hybrids formulated using low- and high-MW chitosan the samples, having bigger pore size, showed lower moisture content probably due to their lower surface area, which decreases the scaffold/water interaction. It is expected that a more opened microstructure would lead to an increased interaction between water vapor pressure at the controlled relative humidity and the scaffold microstructure and so to higher moisture content. Presumably under our experimental conditions the water-scaffold interaction is rather controlled by crosslinking, chitosan MW and possibly due to enhanced hydrogen-bonding interaction between gelatin and high-MW chitosan compared to gelatin and low-MW chitosan rather than by the microstructure of the hybrid scaffolds.

CONCLUSIONS

In this work, synergistic effects of crosslinking and chitosan molecular weight on the microstructure, molecular mobility, thermal and sorption properties of non-crosslinked and crosslinked chitosan/gelatin/hyaluronic acid scaffolds were investigated.

FTIR confirmed the successful crosslinking of chitosan/gelatin/hyaluronic acid scaffolds using EDC/NHS. Detailed pore size analysis of SEM images suggested a synergistic effect when combining crosslinking and the use of low-MW chitosan to obtain porous chitosan/gelatin/hyaluronic acid hybrid scaffolds with relatively large pores. DSC demonstrated that crosslinking of the hybrid scaffold materials along with the use of high-MW chitosan induced a significant increase in T_g. This suggests a reduction in molecular mobility owing to a synergistic effect between crosslinking and the use of high-MW chitosan.

DVS showed that crosslinked chitosan/gelatin/hyaluronic acid scaffolds formulated using high-MW chitosan were found to have reduced moisture contents compared to all hybrid scaffold formulations, showing stronger effect on decreasing moisture content. This means that these scaffolds, when crosslinked and formulated using high-MW chitosan, have low hygroscopic capacity opening interesting characteristic to design packaging for storage processes. In addition, this reduced moisture content effect is highly relevant to provide improved dimensional stability to the scaffolds, which could lead to improved cell behavior including proliferation and differentiation. Future work will focus on studying cell behavior in these scaffolds.

ACKNOWLEDGMENTS

The authors gratefully acknowledge financial support from Conicyt Programa PCI/Newton Picarte Grant N° 140144. J. E., C. A. and F.Q. acknowledge, respectively, financial support from Fondecyt under the Regular Grants N° 1140132 and N° 1160311, and the Postdoctoral Grant N° 3140036.

REFERENCES

1. Tan, H.; Wu, J.; Lao, L.; Gao, C. *Acta Biomater.* **2009**, *5*, 328.
2. Weinstein-Oppenheimer, C.; Aceituno, A.; Brown, D.; Acevedo, C.; Ceriani, R.; Fuentes, M.; Albornoz, F.; Henríquez-Roldán, C.; Morales, P.; Maclean, C.; Tapia, S.; Young, M. *J. Transl. Med.* **2010**, *8*, 1.
3. Yin, Y.; Ye, F.; Cui, J.; Zhang, F.; Li, X.; Yao, K. *J. Biomed. Mater. Res., Part A* **2003**, *67A*, 844.
4. Pant, H. R.; Kim, C. S. *Polym. Int.* **2013**, *62*, 1008.
5. Joy, J.; Gupta, A.; Jahnavi, S.; Verma, R. S.; Ray, A. R.; Gupta, B. *Polym. Int.* **2016**, *65*, 181.
6. Thein-Han, W. W.; Saikhun, J.; Pholpramoo, C.; Misra, R. D. K.; Kitiyanant, Y. *Acta Biomater.* **2009**, *5*, 3453.
7. Ravi Kumar, M. N. V. *React. Funct. Polym.* **2000**, *46*, 1.
8. Pillai, C. K. S.; Paul, W.; Sharma, C. P. *Prog. Polym. Sci.* **2009**, *34*, 641.
9. Hirano, S. *Polym. Int.* **1999**, *48*, 732.
10. Lou, C. W.; Wen, S. P.; Lin, J. H. *J. Appl. Polym. Sci.* **2015**, *132*, 41851.
11. Cañas, A. I.; Delgado, J. P.; Gartner, C. *J. Appl. Polym. Sci.* **2016**, *133*, DOI: 10.1002/app.43814.
12. Mao, J. S.; liu, H. F.; Yin, Y. J.; Yao, K. D. *Biomaterials* **2003**, *24*, 1621.
13. Liu, H.; Mao, J.; Yao, K.; Yang, G.; Cui, L.; Cao, Y. *J. Biomater. Sci., Polym. Ed.* **2004**, *15*, 25.
14. Loh, Q. L.; Choong, C. *Tissue Eng. Part B Rev.* **2013**, *19*, 485.
15. Kovach, I.; Rumschöttel, J.; Friberg, S. E.; Koetz, J. *Colloids Surf. B Biointerfaces* **2016**, *145*, 347.
16. Khorshidi, S.; Solouk, A.; Karkhaneh, A.; Mirzadeh, H.; Sharifi, S.; Mazinani, S. *J. Appl. Polym. Sci.* **2016**, *133*, DOI: 10.1002/app.43832.
17. Podlipec, R.; Gorgieva, S.; Jurašin, D.; Urbančič, I.; Kokol, V.; Štrancar, J. *ACS Appl. Mater. Interfaces* **2014**, *6*, 15980.
18. Keogh, M. B.; O'Brien, F. J.; Daly, J. S. *Acta Biomater.* **2010**, *6*, 4305.
19. Thein-Han, W. W.; Misra, R. D. K. *Acta Biomater.* **2009**, *5*, 1182.
20. Ma, T.; Li, Y.; Yang, S. T.; Kniss, D. A. *Biotechnol. Bioeng* **2000**, *70*, 606.
21. Mecwan, M. M.; Rapalo, G. E.; Mishra, S. R.; Haggard, W. O.; Bumgardner, J. D. *J. Biomed. Mater. Res. Part A* **2011**, *97A*, 66.
22. Fernandes, S. C. M.; Freire, C. S. R.; Silvestre, A. J. D.; Pascoal Neto, C.; Gandini, A. *Polym. Int.* **2011**, *60*, 875.
23. Liu, Z.; Ge, X.; Lu, Y.; Dong, S.; Zhao, Y.; Zeng, M. *Food Hydrocoll.* **2012**, *26*, 311.
24. Enrione, J.; Díaz-Calderón, P.; Weinstein-Oppenheimer, C.; Sánchez, E.; Fuentes, M.; Brown, D.; Herrera, H.; Acevedo, C. *Bioprocess Biosyst. Eng.* **2013**, *36*, 1947.
25. Cai, S.; Zhong, Y.; Li, Y.; Huang, J.; Zhang, J.; Luo, G.; Liu, Z. *PLoS One* **2013**, *8*, e75687.
26. Daniel-da-Silva, A. L.; Salgueiro, A. M.; Trindade, T. *Gold Bull.* **2013**, *46*, 25.
27. Enrione, J. I.; Hill, S. E.; Mitchell, J. R. *J. Agric. Food Chem.* **2007**, *55*, 2956.

28. Roman-Gutierrez, A. D.; Guilbert, S.; Cuq, B. *J. Cereal Sci.* **2002**, *36*, 347.
29. Anderson, R. B. *J. Am. Chem. Soc.* **1946**, *68*, 686.
30. Guggenheim, E. A., Applications of Statistical Mechanics; Clarendon Press: Oxford, **1966**.
31. Boer, J. H., The Dynamical Character of Adsorption; Clarendon Press: Oxford, **1953**.
32. Yan, Z.; Sousa-Gallagher, M. J.; Oliveira, F. A. R. *J. Food Eng.* **2008**, *84*, 359.
33. Liu, H.; Yin, Y.; Yao, K.; Ma, D.; Cui, L.; Cao, Y. *Biomaterials* **2004**, *25*, 3523.
34. Staroszczyk, H.; Sztuka, K.; Wolska, J.; Wojtasz-Pająk, A.; Kołodziejska, I. *Spectrochim. Acta, Part A* **2014**, *117*, 707.
35. Gunasekaran, S.; Anita, B. *Indian J. Pure Appl. Phys.* **2008**, *46*, 833.
36. Lewis, P. D.; Lewis, K. E.; Ghosal, R.; Bayliss, S.; Lloyd, A. J.; Wills, J.; Godfrey, R.; Kloer, P.; Mur, L. A. *J. BMC Cancer* **2010**, *10*, 1.
37. Segal, L. *J. Phys. Chem.* **1961**, *65*, 697.
38. Fripiat, J. J.; Pennequin, M.; Poncelet, G.; Cloos, P. *Clay Miner.* **1969**, *8*, 119.
39. Wang, X. H.; Li, D. P.; Wang, W. J.; Feng, Q. L.; Cui, F. Z.; Xu, Y. X.; Song, X. H.; van der Werf, M. *Biomaterials* **2003**, *24*, 3213.
40. Chiriboga, L.; Xie, P.; Zhang, W.; Diem, M. *Biospectroscopy* **1997**, *3*, 253.
41. Silverstein, R. M.; Webster, F. X.; Kiemle, D.; Bryce, D. L., Spectrometric Identification of Organic Compounds; Wiley: Hoboken, **2014**.
42. Pretsch, E.; Bühlmann, P.; Badertscher, M., Structure Determination of Organic Compounds: Tables of Spectral Data; Springer: Verlag Berlin Heidelberg, **2009**.
43. Acevedo, C.; Somoza, R.; Weinstein-Oppenheimer, C.; Silva, S.; Moreno, M.; Sánchez, E.; Albornoz, F.; Young, M.; MacNaughtan, W.; Enrione, J. *Bioprocess Biosyst. Eng.* **2013**, *36*, 317.
44. García-Pérez, J. V.; Cárcel, J. A.; Clemente, G.; Mulet, A. *LWT – Food Sci. Technol.* **2008**, *41*, 18.